Molecular Crystals and Liquid Crystals
Publication details, including instructions for authors and subscription information:
http://www.tandfonline.com/loi/gmcl20

Dielectric and Optical Studies in Smectic C of A Novel Hydrogen Bonded Liquid Crystal Homologous Series

N. Pongali Sathya Prabu [a] & M. L. N Madhu Mohan [a]
[a] Liquid Crystal Research Laboratory (LCRL), Bannari Amman Institute of Technology, Sathyamangalam, Tamil Nadu, India
Version of record first published: 30 Jul 2012.

To cite this article: N. Pongali Sathya Prabu & M. L. N Madhu Mohan (2012): Dielectric and Optical Studies in Smectic C of A Novel Hydrogen Bonded Liquid Crystal Homologous Series, Molecular Crystals and Liquid Crystals, 562:1, 177-190

To link to this article: http://dx.doi.org/10.1080/15421406.2012.687673

Mol. Cryst. Liq. Cryst., Vol. 562: pp. 177–190, 2012

ISSN: 1542-1406 print/1563-5287 online
DOI: 10.1080/15421406.2012.687673

Taylor & Francis
Taylor & Francis Group

Dielectric and Optical Studies in Smectic C of A Novel Hydrogen Bonded Liquid Crystal Homologous Series

N. PONGALI SATHYA PRABU AND M. L. N MADHU MOHAN*

Liquid Crystal Research Laboratory (LCRL), Bannari Amman Institute of Technology, Sathyamangalam, Tamil Nadu, India

A novel hydrogen bonded liquid crystalline series comprising of p-n alkyloxy benzoic acids is isolated. This series include seven complexes in which hydrogen bond is formed between undecyloxy benzoic acid and various homologues of benzoic acid varying from pentyl to dodecyloxy carbon number. All the homologues of the present series show rich mesomorphism exhibiting orthogonal and tilted phases. The formation of the hydrogen bond is confirmed by Fourier transform infrared spectroscopy studies. Transition temperatures and corresponding enthalpy values along with enantiotropic and monotropic transitions are elucidated from differential scanning calorimetry thermograms. Polarizing optical microscopy revealed various phases in the form of textures. An interesting observation is the identification of a new smectic ordering labeled as smectic X which is sandwiched between traditional nematic and convectional smectic C phases. Dielectric relaxations in smectic C phase of three homologues have been analyzed and the activation energy is calculated from respective Arrhenius plots.

Keywords Arrhenius plots; dielectric relaxations; DSC; smectic X; tilted phases

1. Introduction

Liquid crystals exhibiting the intermediate phases during their phase transitions have both the properties of conventional solid and isotropic liquid which makes these systems unique and gives rise to many interesting properties leading to the engineering application aspects [1]. Molecular orientation and the self-assembly systems form the basic requirements for exhibiting these interesting properties. Hydrogen bonding is one of the principal intermolecular forces which helps in construction of such supra molecular structures and is the key interactions for the chemical and biological processes in nature [2–10]. Recently, a number of supra molecular mesogenic materials have been obtained by molecular self-assembly through intermolecular hydrogen bonding [11–21]. For molecular aggregates, hydrogen bonding plays an important role in the association of the molecules. Kato and his group prepared a variety of liquid crystals induced by this intermolecular hydrogen bonding between pyridyl moieties which are proton acceptors and carboxylic acid groups which are

*Address correspondence to M. L. N Madhu Mohan, Liquid Crystal Research Laboratory (LCRL), Bannari Amman Institute of Technology, Sathyamangalam 638 401, Tamil Nadu, India. Tel.: +91 9442437480; Fax: +91 4295 223775. E-mail: mln.madhu@gmail.com

proton donors [4]. Many liquid crystal systems like molecular liquid crystals [22–26], polymer liquid crystals [27–31], ferroelectric liquid crystals [32,33], and even room temperature liquid crystals have been prepared [8]. Single bond [34–36], double bond [37–40], and even multiple bond [41,42] hydrogen-bonded liquid crystals are synthesized and reported.

The central theme of the aimed research work involves in design, synthesis, and characterization of eight homologous series of hydrogen bonded liquid crystals (HBLC) formed between p-n-alkyloxy benzoic acid (nBAO) and p-n-alkyloxy benzoic acids (mBAO) referred as nBAO+mBAO, where m varies from 5 to 12. These eight series can be referred as 5BAO+mBAO, 6BAO+mBAO, 7BAO+mBAO, 8BAO+mBAO, 9BAO+mBAO, 10BAO+mBAO, 11BAO+mBAO, and 12BAO+mBAO which give rise to 56 different hydrogen-bonded complexes. In this paper, systematic study of the mesogenic properties exhibited by seven complexes of 11BAO+mBAO homologous series are discussed. These system forms the complimentary bond as they themselves behaves as donors and acceptors.

2. Experimental

Optical textural observations were made with a Nikon polarizing optical microscope (POM) equipped with Nikon digital CCD camera system with 5 megapixels and 2560 × 1920 pixel resolutions (Nikon, Tokyo, Japan). The liquid crystalline textures were analyzed and stored with the aid of ACT-2U imaging software system. The temperature control of the liquid crystal cell was equipped by Instec HCS402-STC 200 temperature controller (Instec, Boulder, Colorado) to a temperature resolution of $\pm 0.1^{\circ}$C. This unit was interfaced to computer by IEEE–STC 200 to control and monitor the temperature. The liquid crystal sample was filled by capillary action in its isotropic state into a commercially available (Instec, USA) polyamide buffed cell with 4 μm spacer. Optical extinction technique [40] was used for determination of tilt angle. Transition temperatures and corresponding enthalpy values were obtained by differential scanning calorimetry (DSC) (Shimadzu DSC-60, Kyoto, Japan). Fourier transform infrared spectroscopy (FTIR) spectra was recorded (ABB FTIR MB3000, Quebec, Canada)) and analyzed with the MB3000 software. The p-n-undecyloxy benzoic acid (11BAO) and p-n-alkyloxy benzoic acids (mBAO, where m = 5 to 12) were supplied by Sigma Aldrich (Steinheim, Germany) and all the solvents were of high-performance liquid chromatography (HPLC) grade.

2.1 Synthesis of HBLC

All the inter hydrogen-bonded complexes examined in the present study are prepared by mixing in 1:1 molar ratio undecyloxy benzoic acid with various alkyloxy benzoic acids in dimethyl formamide (DMF) and reprecipitating after the evaporation as described in the reported literature [43–45]. Molecular structure of the present homologous series of p-n-undecyloxy benzoic acid (11BAO) with p-n-alkyloxy benzoic acids (mBAO, Where m = 5 to 12) is depicted in the Fig. 1 where m represents the alkyloxy carbon number.

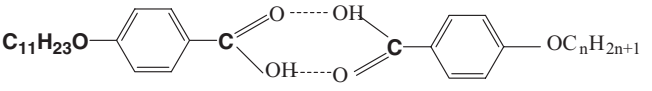

Figure 1. Molecular structure of undecyloxy benzoic acid and alkyloxy benzoic acid hydrogen bonded complexes.

3. Results and Discussion

All the hydrogen-bonded complexes isolated under the present investigation are white crystalline solids and are stable at room temperature (30°C). They are insoluble in water and sparingly soluble in common organic solvents such as methanol, ethanol, benzene, and dichloro methane. However, they show a high degree of solubility in coordinating solvents like dimethyl sulfoxide (DMSO), DMF, and pyridine. All these mesogens melt at specific temperatures below ∼88.4°C (Table 1). They show high thermal and chemical stability when subjected to repeated thermal scans performed during POM and DSC studies.

3.1 Phase Identification

The observed phase variants, transition temperatures, and corresponding enthalpy values obtained by DSC in the cooling and heating cycles for the 11BAO+mBAO complexes are presented in Table 1. These data are in concurrence with POM data.

3.2 Phases Exhibited by 11BAO+nBAO Homologous Series

The mesogens of the p-n-undecyloxy benzoic acid (11BAO) with p-n-alkyloxy benzoic acids (mBAO, where m = 5 to 12) designated as 11BAO+mBAO homologous series are found to exhibit characteristic textures [46], viz., nematic (N) (droplets texture, Plate 1), smectic X (worm like texture, Plate 2), smectic C (schlieren texture, Plate 3), and smectic F (chequered board texture, Plate 4), respectively. The general phase sequence of various homologues of 11BAO+mBAO series in cooling and heating runs can be shown as:

$$Iso \rightleftharpoons N \rightarrow Sm\,X \rightarrow Sm\,C \rightleftharpoons Crystal\,(11BAO{+}5BAO)$$

$$Iso \rightleftharpoons N \rightleftharpoons Sm\,C \rightleftharpoons Crystal\,(11BAO + 6BAO, 7BAO\text{ and }8BAO)$$

$$Iso \rightleftharpoons N \rightarrow Sm\,C \rightleftharpoons Sm\,F \rightleftharpoons Crystal\,(11BAO{+}9BAO)$$

$$Iso \rightleftharpoons N \rightleftharpoons Sm\,C \rightleftharpoons Crystal\,(11BAO{+}10BAO)$$

$$Iso \rightleftharpoons N \rightarrow Sm\,X \rightleftharpoons Sm\,C \rightleftharpoons Crystal\,(11BAO{+}12BAO)$$

Monotropic and enantiotropic transitions are depicted as single and double arrows, respectively.

3.3 FTIR Study

FTIR spectra for all the HBLC complexes are recorded in the solid state (KBr) at room temperature. As a representative case, Fig. 2 illustrates the FTIR spectra of 11BAO+12BAO in solid state at room temperature which is discussed elaborately. It is reported [47,48] that in the alkyloxy benzoic acids, carboxylic acid exists in monomeric form and the stretching vibration of C=O is observed at 1760 cm^{-1}. Further it is known [48] that when a hydrogen bond is formed between carboxylic acids it results in lowering of the carbonyl frequency which has been detected in the present hydrogen-bonded complexes. A noteworthy feature in the spectrum of the 11BAO+12BAO is the appearance of sharp peak at 1674 cm^{-1} which clearly suggests the dimmer formation in particular the carbonyl group vibration [49–51]. A carboxylic acid existing in monomeric form in dilute solution absorbs at about 1760cm^{-1} because of the electron withdrawing effect. However, acids in concentration solution or in solid state tend to dimerize through hydrogen bonding. It is reported [48] that this dimerization weakens the C=O bond and lowers the stretching force constant K,

Table 1. Transition temperatures obtained by different techniques. Enthalpy values (J g^{-1}) given in parenthesis

Carbon	Phase variance	Technique	Crystal melt	N	X	C	F	Crystal
5	NXC	DSC (h)	69.4 (35.94)	141.9 (6.40)	Not resolved	Not resolved		
		DSC (c)		139.2 (5.70)	Not resolved	Not resolved		62.8 (34.29)
		POM (C)		139.9	120.4	119.4		63.1
6	NC	DSC (h)	66.5 (98.83)	143.7 (7.91)		101.2 (1.55)		
		DSC (c)		140.7 (6.93)		99.5 (2.17)		58.4 (38.02)
		POM (C)		141.5		100.1		58.8
7	NC	DSC (h)	68.1 (42.84)	142.5 (6.86)		110.4 (3.27)		
		DSC (c)		139.9 (6.73)		107.9 (3.22)		57.8 (38.84)
		POM (C)		140.5		108.3		57.9
8	NC	DSC (h)	67.5 (40.22)	142.6 (8.75)		118.4 (4.66)		
		DSC (c)		138.9 (7.99)		115.9 (4.28)		63.4 (21.68)
		POM (C)		139.7		116.4		63.7
9	NCF	DSC (h)	76.6 (16.91)	139.6 (8.92)			123.4 (4.77)	
		DSC (c)		136.5 (6.11)		127.9 (1.18)	120.8 (4.47)	71.5 (21.82)
		POM (C)		137.3		128.5	121.2	71.8
10	NC	DSC (h)	88.4 (33.95)	141.1 (10.08)		126.1 (7.53)		88.4 (33.95)
		DSC (c)		138.2 (10.11)		123.0 (6.66)		83.3 (43.34)
		POM (C)		138.9		123.5		83.6
12	NXC	DSC (h)	86.2 (26.18)	139.1 (4.97)	Not resolved	131.3 (7.67)		
		DSC (c)		135.1 (7.25)	Not resolved	127.8 (5.42)		80.7 (33.82)
		POM (C)		135.8	128.3	128.4		80.8

Note: h, heating run; c, cooling run.

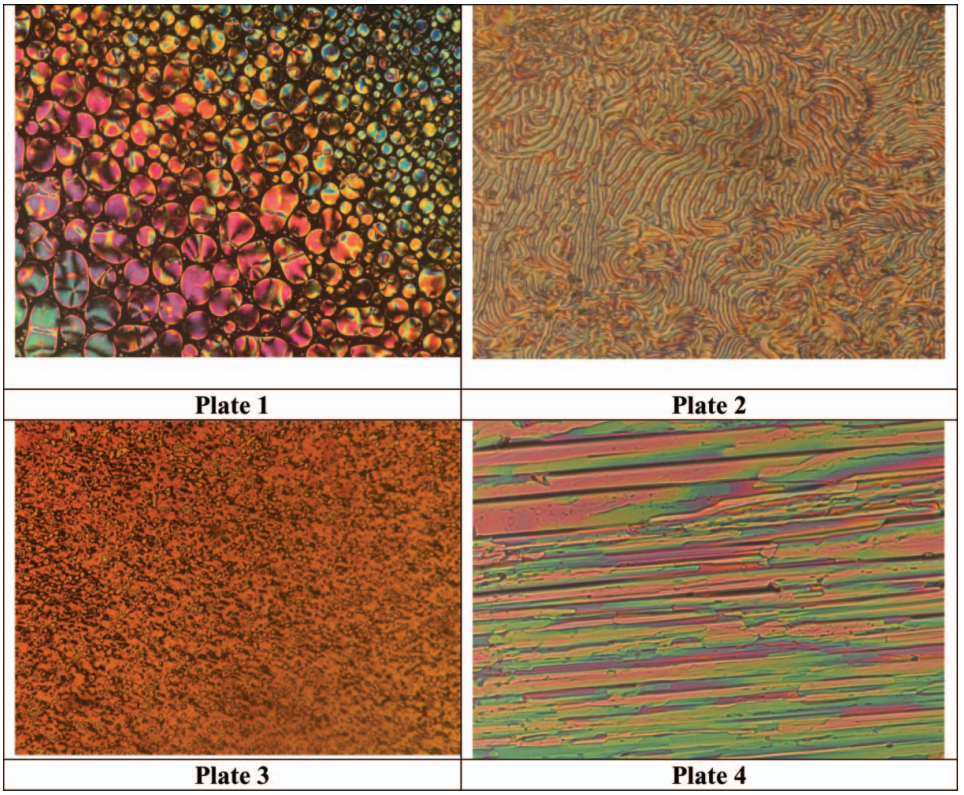

Plates 1–4. 1. Nematic droplets texture of nematic phase obtained in 11BAO+7BAO complex recorded at 125.4°C. **2.** Worm-like texture of smectic X phase obtained in 11BAO+5BAO complex recorded at 120.4°C. **3.** Schlieren texture of smectic C phase obtained in 11BAO+8BAO complex recorded at 105.9°C. **4.** Chequered board texture of smectic F obtained in 11BAO+9BAO complex recorded at 110.7°C. (All plates are recorded under crossed polarizer's with 5 × magnification)

resulting in a lowering of the carbonyl frequency of saturated acids to ∼1710 cm^{-1}. This result concurs with the reported data of Kato et al. [47]. Hence, in the present complexes the formation of H bonding is established by FTIR. A similar trend of result is followed in all the synthesized hydrogen-bonded complexes.

3.4 DSC Studies

DSC thermograms are recorded in heating and cooling cycle. The sample is heated with a scan rate of 10°C min^{-1} and held at its isotropic temperature for 2 min so as to attain thermal stability. The cooling run is performed with the same scan rate of 10°C min^{-1}. The respective equilibrium transition temperatures and corresponding enthalpy values of the mesogens of the homologous series are listed separately in Table 1. POM studies also concur with the DSC transition temperatures. The entire DSC exothermic thermograms of the synthesized 11BAO+mBAO complexes are depicted in Fig. 3. It is plotted for the DSC

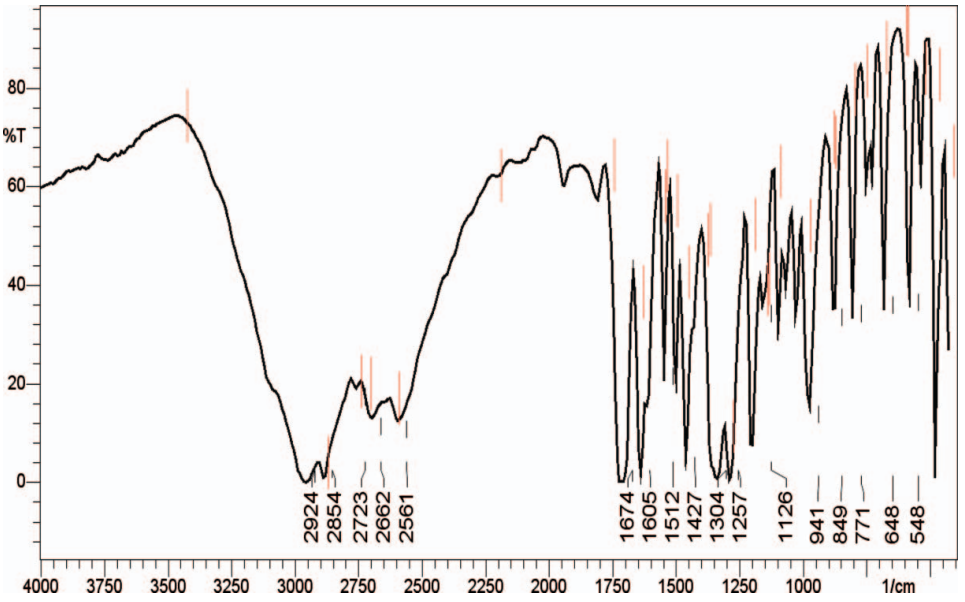

Figure 2. FTIR spectra of 11BAO+12BAO complex.

cooling thermograms by assigning the temperature variation along *x*-axis and the corresponding enthalpy value (ΔH) along *y*-axis. It is inferred from the DSC thermograms (Fig. 3) that as the alkyloxy chain length increases the orthogonal nematic ordering is quenched by the tilted smectic ordering C which paved way for its higher thermal span. Moreover, from the enthalpy values obtained from the cooling run of the DSC thermograms, the phase transitions from isotropic to nematic, nematic to smectic C, and smectic C to crystal is categorized as first-order transitions. In the complexes 11BAO+9BAO, 11BAO+10BAO,

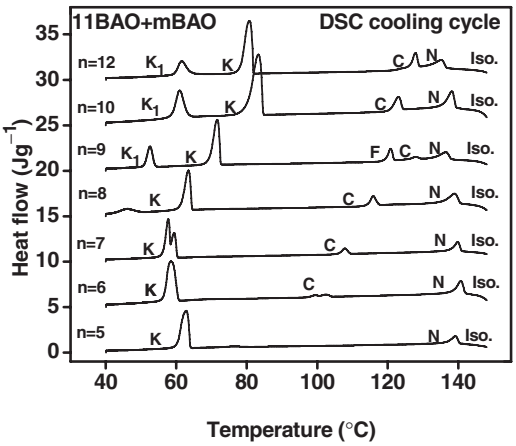

Figure 3. DSC thermogram of 11BAO+mBAO series in cooling run.

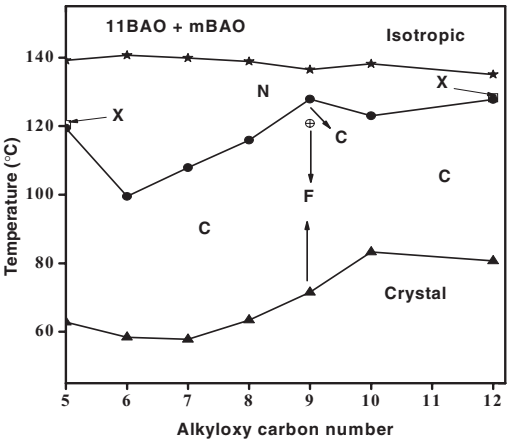

Figure 4. Phase diagram of 11BAO+mBAO homologous series.

and 11BAO+12BAO in the cooling run of the DSC, a transition is noticed after crystallization which is classified as solid-to-solid transition and labeled as K1 (crystal-to-crystal transition).

3.5 Phase Diagram of Pure p-n-alkyloxy Benzoic Acid

The phase diagram of pure 11BAO is reported [52,53] to compose of two phases namely, nematic and smectic C.

3.5.1 Phase Diagram of 11BAO+mBAO. Phase diagram of p-n-undecyloxy benzoic acid and p-n-alkyloxy benzoic acids (11BAO+mBAO) homologues series is depicted in Fig. 4. The following points can be elucidated from Fig. 4:

- The phase diagram consists of four phases, viz. nematic, smectic X, smectic C, and smectic F.
- It is interesting to note that smectic X phase is observed in the first (11BAO+5BAO) and last members (11BAO+12BAO) of the homologous series with a narrow thermal span.
- Nematic and smectic C phases are observed in all the alkyloxy carbon numbers. Quenching of the nematic phase by smectic C is observed as the carbon chain length increases.
- A wide range of thermal span of smectic C is observed in the series.
- A new smectic ordering labeled as Sm X is observed and characterized. In an identical homologous series, a similar phase has been characterized earlier by us [54,55,56] using different techniques.
- It is surprising to note that smectic F, the highly oriented phase is observed only in the 11BAO+9BAO complex.
- The over all mesogenic thermal range possessed by individual complexes of the series has decreased with the increment in carbon number.
- Odd even effect is not observed at isotropic to nematic interface either in transition temperatures or in corresponding enthalpy values.

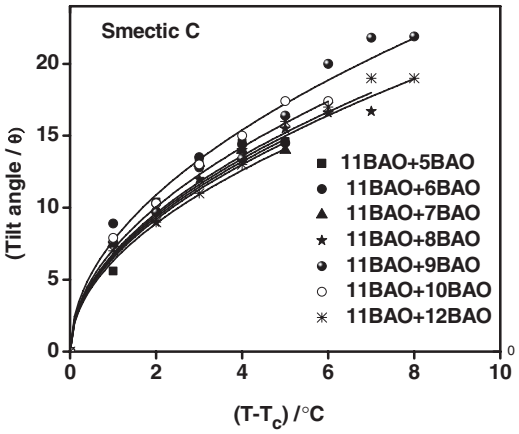

Figure 5. Temperature variation of tilt angle in smectic C phase for 11BAO+mBAO series, where m = pentyloxy to dodecyloxy benzoic acids.

4. Optical Tilt Angle Measurement

The optical tilt angle has been experimentally measured by optical extinction method [40] in smectic C phase for all the members of the present 11BAO+mBAO homologous series. Figure 5 depicts such variation of optical tilt angle with temperature for 11BAO+mBAO (where m = 5 to 12) series. In Fig. 5, the theoretical fit obtained from the mean field theory is denoted by the solid line. It is observed from the figure that the tilt angle increases with decreasing temperature and attains a saturation value. These large magnitudes of the tilt angle are attributed to the direction of the soft covalent hydrogen bond interaction which spreads along molecular long axis with finite inclination [57]. On examining Fig. 5, it can be inferred that in the lower homologues of 11BAO+mBAO (where, m = 5 to 7) the magnitude of saturated tilt angle is observed to be $\sim 14^{\circ}$ while in the higher homologues (m = 8 to 12) the magnitude of saturated tilt angle is observed to be $\sim 18^{\circ}$. This segregation of the complexes based on the magnitude of the tilt angle measured happens to be due to the effective increase in the thermal span of the smectic C phase on suppressing the nematic phase as the alkyloxy chain length is increased. Increase in the carbon number reciprocates an increase in the saturation value of the tilt angle measurement.

Tilt angle is a primary-order parameter [58] and the temperature variation is estimated by fitting the observed data of θ(T) to the relation

$$\theta(\mathrm{T})\alpha(\mathrm{T_C} - \mathrm{T})^{\beta}. \tag{1}$$

The critical exponent β value estimated by fitting the data of θ(T) to the above equation (1) is found to be 0.50 to agree with the mean field prediction [1,59]. The solid lines in the Fig. 5 depict the fitted data for various mesogens. Further, the agreement of magnitude of β (0.5) with mean field value (0.5) infers the long-range interaction of transverse dipole moment for the stabilization of tilted smectic C phase.

5. Dielectric Studies

Empty cell is calibrated with temperature (30°C–200°C) and frequency (5Hz–13 MHz) by a known substance (benzene) to calculate the leads capacitance.

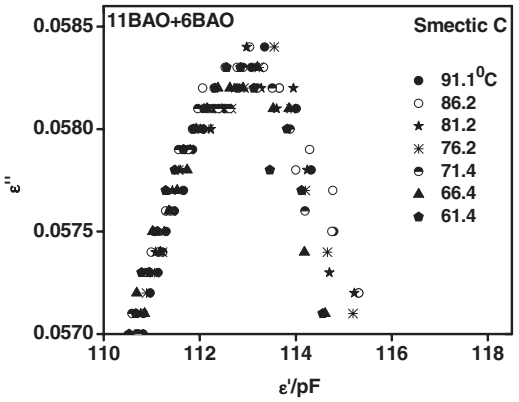

Figure 6. Dispersion curves obtained for the 11BAO+6BAO complex in its smectic C phase for various temperatures.

5.1 Dielectric Relaxations

Dielectric dispersion, i.e., frequency variation of dielectric loss exhibited by 11BAO+ 6BAO, 11BAO+7BAO, and 11BAO+8BAO are studied at different temperatures in smectic C phase in the frequency range of 5–13 MHz. An impedance analyzer (Agilent 4192A LF, Santa Clara, California) is operated with $1V_{P\text{-}P}$ oscillating signal with zero-bias field. Relative permittivity $\varepsilon'_r(\omega)$ and dielectric loss $\varepsilon''(\omega)$ are calculated by the following equations

$$^*\varepsilon'_r(\omega) = \varepsilon'_r(\omega) - j\varepsilon''(\omega),$$

$$\varepsilon'_r(\omega) = [C_{LC} - C_{leads}]/[C_{empty} - C_{leads}],$$

$$^*\varepsilon'_r(\omega) = \mathrm{Tan}\delta(\omega)^*\varepsilon_r(\omega).$$

To detect the possible relaxation in the 11BAO+nBAO complexes, the mesogens are scanned in the frequency range of 5–13 MHz at different temperatures in the smectic C phase of the corresponding complex. In all the complexes the relaxation frequency (f_r) decreases with lowering temperature which is suggestive of an Arrhenius behavior [60–62] as it reflects the collective response. Further, the magnitude of the dielectric loss is shifted and is not suppressed by the temperature the slope of the log of relaxation frequency to inverse of temperature, referred as Arrhenius plot gives the activation energy of the phase. The high value of the activation energies in complexes is attributed to the steric hindrance of the alkyloxy benzoic acid moiety.

The corresponding dispersion curves and Arrhenius plots for all the complexes studied are illustrated in Figs 6–9 and they appear to be asymmetric about ε''_{max}. Such a asymmetric non-Debbie's type of off-centered dispersion is studied by Cole–Davidson theory [60–62] given by

$$\varepsilon''(\omega) = \{\varepsilon_\infty - [(\Delta\varepsilon)]/[1 + (j\omega\tau)^{1-\alpha}\},$$

where

$\Delta\varepsilon = (\varepsilon_o - \varepsilon_\infty) =$ the dielectric increment (strength),
$\omega = 2\pi f$ (where f is the frequency of AC signal),

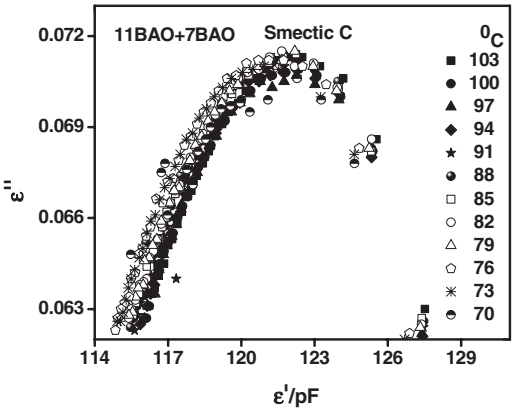

Figure 7. Dispersion curves obtained for the 11BAO+7BAO complex in its smectic C phase for various temperatures.

T = relaxation time, i.e., 1 f_r^{-1},

α = the distribution parameter (or degrees of freedom) to estimate the influence of environment of dipoles and its fixation in the molecular frame during the reorientation to the field.

5.1.1 Dielectric Relaxations in 11BAO+6BAO. The dielectric relaxations in 11BAO+ 6BAO complex have been investigated in the entire thermal span of smectic C phase (99.5°C to 58.5°C) at seven temperatures namely 91.1°C, 86.2°C, 81.2°C, 76.2°C, 71.4°C, 66.4°C, and 61.4°C, respectively, which are decremented in equal steps of 5°C.

The shift of the relaxation frequency (f_r) to lower side with decrease in temperature can be noticed from Fig. 6 and Table 2. The relaxation frequency shifted from 225 KHz to 210 KHz in a temperature span of 30°C. Arrhenius plots are drawn (Fig. 9) and the activation energy corresponding to smectic C is calculated to be 0.95 eV. Table 2 presents the studied temperatures, the magnitudes of relaxation frequency, dielectric loss, and corresponding

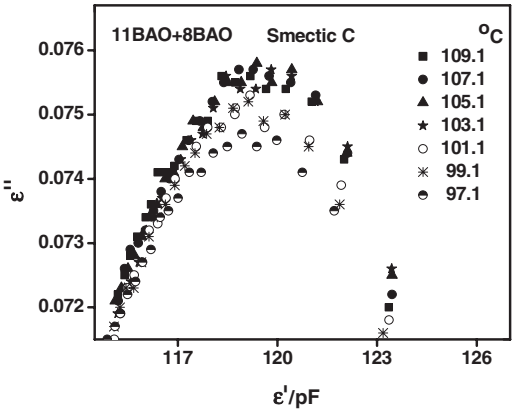

Figure 8. Dispersion curves obtained for the 11BAO+8BAO complex in its smectic C phase for various temperatures.

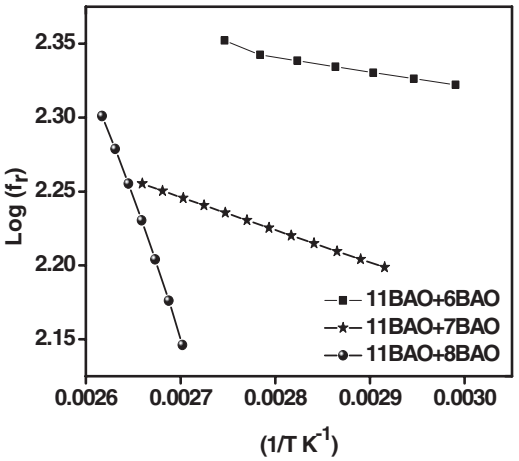

Figure 9. Arrhenius plots for 11BAO+mBAO complexes (m = 6 to 8).

Table 2. Values of relaxation frequency and corresponding temperature along with activation energy for various complexes

Complex	T (°C)	f_r (KHz)	τ (μs)	ε'' max	α (rad)	Activation energy (eV)
11BAO+6BAO	91.1	225	4.44	0.0583	0.8198	0.95
	86.2	220	4.54	0.0583	0.7152	
	81.2	218	4.58	0.0582	0.628	
	76.2	216	4.62	0.0581	0.5931	
	71.4	214	4.67	0.0581	0.5582	
	66.4	212	4.71	0.0581	0.5233	
	61.4	210	4.76	0.0580	0.3663	
11BAO+7BAO	103	180	5.55	0.0719	0.2965	0.99
	100	178	5.61	0.0718	0.3663	
	97	176	5.68	0.0717	0.5233	
	94	174	5.74	0.0716	0.5407	
	91	172	5.81	0.0715	0.5582	
	88	170	5.88	0.0714	0.6105	
	85	168	5.95	0.0713	0.6628	
	82	166	6.02	0.0712	0.6977	
	79	164	6.09	0.0710	0.7326	
	76	162	6.17	0.0708	0.7501	
	73	160	6.25	0.0707	0.8024	
	70	158	6.32	0.0706	0.8198	
11BAO+8BAO	109.1	200	5	0.0758	0.8547	0.99
	107.1	190	5.26	0.0757	0.8024	
	105.1	180	5.55	0.0756	0.7850	
	103.1	170	5.88	0.0755	0.4361	
	101.1	160	6.25	0.0751	0.4136	
	99.1	150	6.66	0.0750	0.4012	
	97.1	140	7.14	0.0747	0.3837	

relaxation time. The distribution parameter α has been calculated for each relaxation process and it is noticed that the magnitude of α decreases as the temperature is decreased.

5.1.2 Dielectric Relaxations in 11BAO+7BAO. The dielectric relaxations in 11BAO+ 7BAO complex have been investigated in the entire thermal span of smectic C phase (107.9°C to 57.9°C) at 12 temperatures namely 103°C, 100°C, 97°C, 94°C, 91°C, 88°C, 85°C, 82°C, 79°C, 76°C, 73°C, and 70°C, respectively, which are decremented in equal steps of 3°C. The shift of the relaxation frequency (f_r) to lower side with decrease in temperature can be noticed from Fig. 7 and Table 2. The relaxation frequency shifted from 180 KHz to 158 KHz in a temperature span of 33°C. Arrhenius plots are drawn (Fig. 9) and the activation energy corresponding to smectic C is calculated to be 0.99 eV. Table 2 presents the studied temperatures, the magnitudes of relaxation frequency, dielectric loss, and corresponding relaxation time. The distribution parameter α has been calculated for each relaxation process and it is noticed that the magnitude of α increases as the temperature is decreased.

5.1.3 Dielectric Relaxations in 11BAO+8BAO. The dielectric relaxations in 11BAO+ 8BAO complex have been investigated in the entire thermal span of smectic C phase (115.9°C to 63.5°C) at seven temperatures namely 109.1°C, 107.1°C, 105.1°C, 103.1°C, 101.1°C, 99.1°C, and 97.1°C, respectively, which are decremented in equal steps of 2°C. The shift of the relaxation frequency (f_r) to lower side with decrease in temperature can be noticed from Fig. 8 and Table 2. The relaxation frequency shifted from 200 KHz to 140 KHz in a temperature span of 12°C. Arrhenius plots are drawn (Fig. 9) and the activation energy corresponding to smectic C is calculated to be 0.99 eV. Table 2 presents the temperatures studied the magnitudes of relaxation frequency, dielectric loss, and corresponding relaxation time. The distribution parameter α has been calculated for each relaxation process and it is noticed that the magnitude of α decreases as the temperature is decreased.

Acknowledgments

The graceful blessings showered by the goddesses Bannari Amman are gratefully acknowledged. Infrastructural support provided by Bannari Amman Institute of Technology is also gratefully acknowledged.

References

[1] Chandrasekhar, S. (1977). *Liquid Crystals*, Cambridge University Press: Cambridge, London.
[2] Kato, T., & Frechet, J. M. J. (1995). *Macromol. Symp.*, *98*, 311.
[3] Paleos, C. M., & Tsiourvas, D. (1995). *Angew. Chem., Int. Ed. Engl.*, *34*, 1696.
[4] Kato, T., & Frechet, J. M. J. (1989). *J. Am. Chem. Soc.*, *111*, 8533.
[5] Kato, T., Fujishima, A., & Frechet, J. M. J. (1990). *Chem. Lett.*, *19*, 919.
[6] Kato, T., Frechet, J. M. J., Wilson, P. G., Saito, T., Uryu, T., Fujishima, A., Jin, C., & Kaneuchi, F. (1993). *Chem.Mater.*, *5*, 1094.
[7] Kato, T., Kihara, H., Kumar, U., Uryu, T., & Frechet, J. M. J. (1994). *Angew. Chem., Int. Ed. Engl.*, *33*, 1644.
[8] Kato, T., Fukumasa, M., & Frechet, J. M. J. (1995). *Chem. Mater.*, *7*, 368.
[9] Kato, T., Nakano, T., Moteki, M., & Uryu, T. (1995). *Macromolecules*, *28*, 8875.
[10] Kato, T., Kubota, Y., Nakano, M., & Uryu, T. (1995) *Chem. Lett.*, *161*, 1127.
[11] Lehn, J. M.,(1993). *Macromol. Symp.*, *69*, 1.
[12] Fouquey, C., Lehn, J. M., & Levelut, A. M. (1990). *Adv. Mater.*, *2*, 254.

[13] Bruce, D. W., & Price, D. J. (1994). *Adv. Mater. Opt. Electron.*, *4*, 273.
[14] Willis, K., Price, D. J., Adams, H., Unger, G., & Bruce, D. W. (1995). *J. Mater. Chem.*, *5*, 2195.
[15] Sato, A., Kato, T., & Uryu, T. (1996). *J. Polym. Sci.*, *34*, 503.
[16] Malik, S., Dhal, P. K., & Mashelkar, R. A. (1995). *Macromolecules*, *28*, 2159.
[17] Xu, B., & Swager, T. M. (1995). *J. Am. chem. Soc.*, *117*, 5011.
[18] Kumar, U., Frechet, J. M. J., Kato, T., Ujie, S., & Imura, K. (1992). *Angew. Chem., Int. Ed. Engl.*, *31*, 1531.
[19] Kato, T., Kihara, H., Uryu, T., Ujiie, S., Imura, K., Frechet, J. M. J., & Kumar, U. (1993). *Ferroelectrics*, *148*, 161.
[20] Kato, T., Kihara, H., Uryu, T., Fujishima, A., & Frechet, J. M. J. (1992). *Macromolecules*, *25*, 6836.
[21] Kato, T., Uryu, T., Kaneuchi, F., Jin, C., & Frechet, J. M. J. (1993). *Liq. Cryst.*, *14*, 1311.
[22] Kato, T., Wilson, P. G., Fujishima, A., & Frechet, J. M. J. (1990). *Chem. Lett.*, *19*, 2003.
[23] Kato, T., Adachi, H., Fujishima, A., & Frechet, J. M. J. (1992). *Chem. Lett.*, *21*, 265.
[24] Yu, L. J., Wu, J. M., & Wu, S. L. (1991). *Mol. Cryst. Liq. Cryst.*, *198*, 407.
[25] Sideratou, Z., Paleos, C. M., & Skoulios, A. (1995). *Mol. Cryst. Liq. Cryst.*, *19*, 265.
[26] Yu, L. J., & Pan, J. S. (1993). *Liq. Cryst.*, *13*, 829.
[27] Kato, T., & Frechet, J. M. J. (1989). *Macromolecules*, *22*, 3816.
[28] Kumar, U., Kato, T., & Frechet, J. M. J. (1992). *J. Am. Chem. Soc.*, *114*, 6630.
[29] Wilson, L. M.,(1994). *Macromolecules*, *27*, 6683.
[30] Alexander, C., Jariwala, C. P., Lee, C. M., & Griffin, A.C. (1993). *Polymer Reprints*, *34*, 168.
[31] Alexander, C., Jariwala, C. P., Lee, C. M., & Griffin, A. C. (1994). *Die Makromol. chem. Macromol. symp.*, *77*, 283.
[32] Yu, L. J. (1993). *Liq. Cryst.*, *14*, 1303.
[33] Tian, Y. Q., Su, F. Y., Shao, Y. Y., Lu, X. Y., Tang, X. Y., Zhao, X. G. & Zhou, E. L. (1995). *Liq. Cryst.*, *19*, 743.
[34] Pongali Sathya Prabu, N., Vijayakumar, V. N., & Madhu Mohan, M. L. N. (2011). *J. Mol. Str.*, *994*, 387.
[35] Pongali Sathya Prabu, N., Vijayakumar, V. N., & Madhu Mohan, M. L. N. (2011). *Physica B:Soft condensed matter*, *406*, 1106.
[36] Pongali Sathya Prabu, N., Vijayakumar, V. N., & Madhu Mohan, M. L. N. (2011). *Mol. Cryst. Liq. Cryst.*, *548*, 154.
[37] Vijayakumar, V. N., & Madhu Mohan, M. L. N. (2009). *J. Opto. Elec. Adv. Mat.*, *11*, 1139.
[38] Vijayakumar, V. N., & Madhu Mohan, M. L. N. (2009). *Braz. J. Phy.*, *39*, 677.
[39] Vijayakumar, V. N., Murugadass, K., & Madhu Mohan, M. L. N. (2009). *Braz. J. Phy.*, *39*, 600.
[40] Vijayakumar, V. N., & Madhu Mohan, M. L. N. (2009). *Sol. State. Comm.*, *149*, 2090. Federal Republic of Germany.
[41] Lehn, J. M. (1995). *Concept and Perspectives*, VCH Weinheim.
[42] Fouquey, C., Lehn, J. M., & Mlevelut, A. (1990). *Adv. Mater.*, *2*, 254.
[43] Kato, T., & Frechet, J. M. J. (1989). *J. Am. Chem. Soc.*, *111*, 8533.
[44] Kato, T., & Frechet, J. M. J. (1995). *Macromol. Symp.*, *95*, 311.
[45] Kato, T., & Frechet, J. M. J. (1989). *Macromolecules*, *22*, 3818.
[46] Gray, G. W., & Goodby, J. W. G. (1984). *Smectic Liquid Crystals: Textures and Structures*, Leonard Hill: London.
[47] Kato, T., Uryu, T., Kaneuchi, F., Jin, C., & Frechet, J. M. J. (1993). *Liq. Cryst.*, *14*, 1311.
[48] Pavia, D. L., Lampman, G. M., & Kriz, G. S. (2007). *Introduction to spectroscopy*, Sanat Printers: Kundli, India.
[49] Nakamoto, K. (1978). *Infrared and Raman Spectra of Inorganic and Co-ordination Compounds*, Interscience: New York.
[50] Xu, J. (2006). *J. Mater. Chem.*, *16*, 3540.
[51] Frechet, J. M. J., & Kato, T. (1992). US Patent No 5139696.
[52] Srinivasulu, M., Satyanarayana, P. V. V., Kumar, P. A., & Pisipati, V. G. K. M. (2002). *Z. Naturforsch., A: Phys. Sci.*, *56*, 685.

[53] Swathi, P., Kumar, P. A., Pisipati, V. G. K. M., Rajeswari, A. V., Sreehari Sastry, S., & Narayana Murty, P. (2002). *Z. Natur Forsch.*, *57*, 797.
[54] Vijayakumar, V. N., Murugadass, K., & Madhu Mohan, M. L. N. (2010). *Mol. Cryst. Liq. Cryst.*, *517*, 43.
[55] Vijayakumar, V. N., & Madhu Mohan, M. L. N. (2009). *Ferroelectrics*, *392*, 81.
[56] Vijayakumar, V. N., & Madhu Mohan, M. L. N. (2010). *Z. Naturforsch.*, *65*, 1156.
[57] Barmatov, E. B., Bobrovsky, A., Barmatova, M. V., & Shibaev, V. P. (1999). *Liq. Cryst.*, *26*, 581.
[58] De Gennes, P. G. (1974). *The Physics of Liquid Crystals*, Oxford Press: London.
[59] Stanley, H. E. (1971). *Introduction to Phase Transition and Critical Phenomena*, Clarendon Press: New York.
[60] Hills, N. E., Wanghan, W. E., Price, A. H., & Davies, M. (1969). *Dielectric Properties and Molecular Behavior*, Vannostrand: New York.
[61] Jonscher, A. H. (1983). *Dielectric Relaxation in Solids*, Chelsea Dielectric Press: London.
[62] Cole, R. H. (1941). *J. Chem. Phys.*, *9*, 341.